51st IEEE Conference on Decision and Control
December 10-13, 2012. Maui, Hawaii, USA

Green Scheduling for Radiant Systems in Buildings

Truong X. Nghiem, Madhur Behl, George J. Pappas and Rahul Mangharam
Department of Electrical and Systems Engineering
University of Pennsylvania
{nghiem, mbehl, pappasg, rahulm}@seas.upenn.edu

Abstract— **In this paper we look at the problem of peak power reduction for buildings with electric radiant floor heating systems. Uncoordinated operation of a multi-zone radiant floor heating system can result in temporally correlated electricity demand surges or peaks in the building's electricity consumption. As peak power prices are 200-400 times that of the nominal rate, this uncoordinated activity can result in high electricity costs and expensive system operation. We have previously presented green scheduling as an approach for reducing the aggregate peak power consumption in buildings while ensuring that indoor thermal comfort is always maintained. This paper extends the theoretical results for general affine dynamical systems and applies them to electric radiant floor heating systems. The potential of the proposed method in reducing the peak power demand is demonstrated for a small-scale system through simulation in EnergyPlus and for a large-scale system through simulation in Matlab.**

I. Introduction

Commercial electricity customers are often subject to peak-demand based electricity pricing [1]. In this pricing policy, a customer is charged not only for the amount of electricity it has consumed but also for its maximum demand over the billing cycle. The unit price of the peak demand charge is usually very high, up to 240 times in some cases [2] and even more. This is to discourage the use of electricity under peak load conditions since they can cause issues such as low quality of service and service disruptions, which affect the reliability of the grid. High peak loads also lead to a higher cost of production and distribution of electricity. Therefore, peaks in electricity usage are inefficient and expensive for both suppliers and customers.

In this paper we look at the problem of peak demand reduction for buildings with electric radiant floor heating systems. Uncoordinated operation of a multi-zone radiant floor heating system in a building can result in temporally correlated electricity demand surges (or peaks) leading to high electricity cost under the peak-demand pricing policy.

Radiant floor heating systems serve as an alternative to the conventional forced-air heating, ventilation and air conditioning (HVAC) systems for buildings. Nowadays, these systems are widely used in both commercial and residential buildings in Korea, Germany, Austria, Denmark [3] and in some parts of the United States [4]. The benefits of radiant systems over forced-air HVAC systems for US commercial buildings has been studied in [5].

There exist several different approaches to balance the power consumption in buildings and avoid peaks, e.g., by load shifting and load shedding [6], [7]. However, they operate on coarse grained time scales and do not guarantee any thermal comfort. Another popular approach to energy efficient control for commercial buildings and data centers is model predictive control (MPC) ([8], [9]). In [8] the authors investigated MPC for thermal energy storage in building cooling systems. Peak electricity demand reduction by MPC with real-time pricing was considered in [9]. In [10] MPC is used for achieving energy savings for a hydronic central heating system.

Several improvements over the on/off control for radiant systems have been proposed in literature ([11], [12], [13], [14]). Predictive control methods were shown in [11], [12] to improve the comfort of radiant systems. A two-parameter switching control strategy was described in [13] and was shown to achieve better temperature regulation than on/off control. In [14], three different strategies for control of multi-zone hydronic radiant systems were compared. In all of the above work, the focus has been on improving the thermal comfort of radiant floor systems by achieving better temperature regulation. *Mostly, the simulations and experimental tests have been limited to a single zone*. For the few papers that deal with radiant systems in multiple zones ([12], [14]), the problem of reducing the peak power, which is the focus of our work, has not been addressed.

In our recent paper [15] we proposed *green scheduling* as an approach to schedule the building control systems and reduce the aggregate peak power demand while ensuring that indoor thermal comfort is always maintained. However, the results were developed for simple zone models with no thermal interactions between the zones. The contributions of this paper, compared to our previous work [15], are threefold:

1) We extend the schedulability analysis and scheduling synthesis for general affine dynamical systems with inter-system interactions, and apply them to electric radiant floor heating systems;
2) We use a more accurate system model which incorporates the thermal dynamics of radiant heating systems, the thermal dynamics of zones, and the thermal interactions between zones;
3) We demonstrate the potential of our approach in reducing the peak demand through simulations in EnergyPlus for realistic building radiant system models.

This paper is organized as follows. First, we present an overview of radiant heating systems and their dynamics, and formulate the peak demand reduction problem in Section II. In Section III the generalized green scheduling problem is discussed followed by the schedulability analysis. A method

This material is based upon work supported by the DoE Energy Efficient Buildings (EEB) HUB sponsored by the U.S. Department of Energy under Award Number DE-EE0004261.

978-1-4673-2066-5/12/$31.00 ©2012 IEEE

for synthesizing periodic schedules for the system is proposed in Section IV. Section V describes two simulation case studies and shows the effectiveness of our method for reducing the peak power consumption. Finally, we conclude the paper with a discussion in Section VI.

II. Radiant floor heating systems

A conventional forced-air HVAC system uses the flow of air to provide thermal comfort within a conditioned space. HVAC systems rely on ductwork, vents, etc. as means of air distribution and use air handlers, filters, blowers, heat exchangers, and various controls to regulate the temperature and flow of air entering a space.

On the other hand, radiant heating systems involve supplying heat directly to the floor or to panels in the walls or ceiling of a house. A radiant floor heating system works by warming up the floor surface which then slowly radiates heat upward into the living space, rather than blowing around the heated air. This natural heat transfer is both more comfortable and energy efficient [3]. Furthermore, radiant heating systems also minimize drafts and dust movements, thereby providing a clean and quiet operation [16].

Modern floor heating systems use either electrical resistance elements or fluid flowing in pipes to heat the floor [16]. Hydronic radiant floor systems pump hot water through tubing laid in a pattern underneath the floor. Electric radiant floors typically consist of electric cables (heating elements) built into the floor. Whether cables or tubing, the operation of electric and hydronic radiant systems in floors is the same. Cables or tubing are embedded within the solid floor having a high thermal capacity. If the floor's thermal mass is large enough, the thermal energy stored in it keeps the space conditioned for several hours.

A. Radiant floor model

We consider $m > 1$ zones. Each zone i is equipped with an electric radiant floor heating system with a maximum power rating of q_i (kW). The actuation of each radiant system is assumed to be on-off, i.e., it can be either switched on, when it provides heating power q_i, or switched off, when it provides no heating power. Thus the control input to zone i is a binary variable $u_i \in \{0, 1\}$, where $u_i = 0$ corresponds to the off state and $u_i = 1$ the on state. The floor of each zone consists of a slab of high thermal capacity below which the radiant heat source is embedded. The dynamics of each zone is modeled using an RC network model as shown in Figure 1. The list of parameters in the model is given in Table I. Each zone i has 4 nodes: $T_{g,i}$ is the ground temperature, $T_{sb,i}$ the temperature of the bottom surface of the slab, $T_{st,i}$ the temperature of the top surface of the slab, and T_i the zone air temperature (the air in the zone is assumed to be fully mixed). It is assumed that the slab is uniformly heated and there is no lateral temperature difference or heat transfer. For each zone i, the heat transfer between the ground, the slab and the zone is modelled using equations of one dimensional heat conduction [17]:

$$C_{s,i}\frac{\mathrm{d}T_{sb,i}}{\mathrm{d}t} = K_{g,i}(T_{g,i} - T_{sb,i}) + K_{s,i}(T_{st,i} - T_{sb,i}) + q_i u_i \quad (1)$$

$$C_{s,i}\frac{\mathrm{d}T_{st,i}}{\mathrm{d}t} = K_{a,i}(T_i - T_{st,i}) + K_{s,i}(T_{sb,i} - T_{st,i}). \quad (2)$$

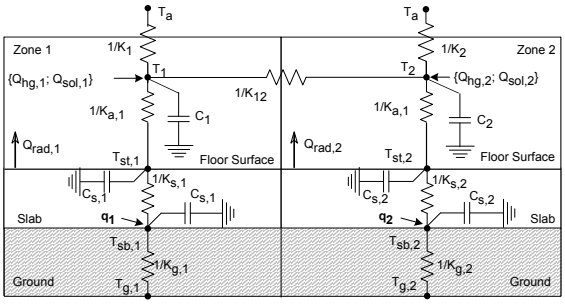


Fig. 1. RC network model for an electric floor heating system for 2 zones.

TABLE I

List of parameters

$K_{g,i}$	conduction coefficient between ground and slab (kW/K)
$K_{a,i}$	convection coefficient between the slab and air (kW/K)
$K_{s,i}$	thermal resistance of the slab (kW/K)
$C_{s,i}$	thermal capacitance of the slab (kJ/K)
C_i	thermal capacitance of zone i (kJ/K)
K_i	thermal conductance between zone i and outside air (kW/K)
K_{ij}	thermal conductance between zone i and zone j (kW/K)

B. Zone model

Let T_a be the ambient air temperature (°C), which is the same for all zones. For zone i, let $Q_{hg,i}$ be its internal heat gain (kW) (from its occupants, equipment, lighting, etc.), and $Q_{sol,i}$ be the heat gain due to solar radiation (kW). We consider T_a, $Q_{hg,i}$ and $Q_{sol,i}$ as disturbances. From the law of conservation of energy, we have for each zone i

$$C_i\frac{\mathrm{d}T_i(t)}{\mathrm{d}t} = K_i\left(T_a(t) - T_i(t)\right) + \textstyle\sum_{j\neq i} K_{ij}\left(T_j(t) - T_i(t)\right) + K_{a,i}(T_{st,i} - T_i) + Q_{hg,i}(t) + Q_{sol,i}(t) \quad (3)$$

where C_i, K_i, and K_{ij} are parameters given in Table I.

The differential equations (1) to (3) of the radiant floor model and the zone model for all the zones can be combined to give a state-space model of the entire system:

$$\dot{x}(t) = Ax(t) + Bu(t) + Hw(t), \quad y(t) = Cx(t). \quad (4)$$

Here, the state vector x consists of the node temperatures for all zones, i.e., $x = [T_{sb,1}, T_{st,1}, T_1, \ldots, T_{sb,m}, T_{st,m}, T_m]^T$; $u = [u_1, \ldots, u_m]^T$ is the binary control input vector to the zones; $w = [T_a, Q_{hg,1}, Q_{sol,1}, \ldots, Q_{hg,m}, Q_{sol,m}]^T$ is the vector of all disturbances; and $y = [T_1, \ldots, T_m]^T$ is the output vector of all zone air temperatures. It is straightforward to see that the state matrix A is a strictly diagonally dominant matrix with negative diagonal entries. Therefore A is Hurwitz [18] and the system is always stable.

C. Peak demand reduction problem

At any time t, the aggregate demand Q of all radiant heating systems is the sum of their individual power demands: $Q(t) = \sum_{i=1}^{m} q_i u_i(t)$. As mentioned in Section I, reducing the peak demand over the billing cycle helps save energy as well as the highly priced demand charge. Thus, the objective of peak demand reduction is to minimize, or reduce, the peak demand $\max_{0\leq t\leq t_f} Q(t)$. However, it must also maintain the indoor thermal comfort in each zone, which requires that the air temperature T_i in zone i should be in a range $[l_i, h_i]$ (°C), e.g., between 22 °C and 24 °C. Therefore, the peak demand reduction problem can be formally stated as follows.

Peak demand reduction problem: *Compute control input $u(t)$, $0 \le t \le t_f$, for system* (4) *to minimize the peak demand while maintaining thermal comfort in each zone.*

In [15], we described *green scheduling* to reduce the peak demand of a large number of heating systems. This was achieved by coordinating the individual systems under a constrained peak while ensuring that custom climate conditions are facilitated. In particular, the peak demand is restricted by requiring that at most k of the m actuators, for $1 \le k \le m$, can be on simultaneously. Applying the green scheduling approach to peak demand reduction for radiant heating systems results in the following problem.

Green scheduling problem for radiant heating systems: *Given a peak constraint $1 \le k \le m$, compute control input $u(t)$, $0 \le t \le t_f$, for system* (4) *so that $\sum_{i=1}^{m} u_i(t) \le k$ at all time while maintaining thermal comfort in each zone.*

In the next section, we generalize the results in [15] to affine dynamical systems that capture the radiant system model (4). A procedure to synthesize periodic control inputs for the green scheduling problem is presented in Section IV.

III. Green scheduling for affine systems

A. System model for green scheduling

We first generalize the state-space model (4) of radiant heating systems for green scheduling. The disturbances w in (4) usually vary slowly. Thus, we can assume constant nominal values $\overline{w}$ for w, and adjust the model for green scheduling in real-time based on either prediction of disturbances (e.g., weather forecast, occupancy schedule) or monitoring of the environment. Therefore the system model for green scheduling is an affine dynamical model:

$$\dot{x}(t) = Ax(t) + (Bu(t) + B_0), \quad y(t) = Cx(t). \qquad (5)$$

Here, $x \in \mathbb{R}^n$ are the states, $u \in \{0,1\}^m$ the binary control inputs, and $y \in \mathbb{R}^p$ the outputs. Matrix $A \in \mathbb{R}^{n \times n}$ is Hurwitz. Vector $B_0 \in \mathbb{R}^n$ corresponds to the nominal disturbances: from (4) we have $B_0 = H\overline{w}$.

Operation specifications, e.g., thermal comfort, require that the outputs y should be in a *safe set* $\texttt{Safe} \subseteq \mathbb{R}^p$. Safe is usually a hyper-rectangle of the form $[l_1, h_1] \times \cdots \times [l_p, h_p]$, but it can also be any convex set.

A control signal $u(\cdot)$ for (5) can be thought of as a schedule that switches on-off and coordinates the individual systems. In this paper, we will use the terms *control signal* and *schedule* interchangeably for $u(\cdot)$. If $u(\cdot)$ drives the system's outputs to Safe and maintains them in that set then the system is said to be *safe* and $u(\cdot)$ is a *safe schedule*. More precisely, the system is *safe* with $u(\cdot)$ if for any initial state $x(0)$, there exists a finite time $\tau \ge 0$ such that $y(t) \in \texttt{Safe}$ for all $t \ge \tau$. In the green scheduling approach the actuators u_i are coordinated so that at any time, at most k of them, for some given $1 \le k \le m$, can be on simultaneously. The system is said to be *k-schedulable* if there exists a safe schedule $u(\cdot)$ such that $\sum_{i=1}^{m} u_i(t) \le k$ for all $t \ge 0$.

Our previous analysis in [15] assumed that each individual system is modeled by a single state variable (which is also its output) and they are decoupled (no heat transfer between zones) so that A is diagonal. This paper makes a major generalization by removing both restrictions, therefore making the model capture the actual systems more accurately.

B. Schedulability analysis

A fundamental question of the green scheduling problem is *k-schedulability*, that is on which conditions the system is k-schedulable for a given k. The answer to this question will allow us to find an appropriate peak constraint k. In our previous work [15], k-schedulability conditions were obtained for systems with simpler dynamics by showing the existence of periodic control signals that satisfy the peak constraint and drive the system to the safe set. Along the same line, in this paper, we investigate periodic control signals for system (5) to derive sufficient conditions for the system to be k-schedulable.

A T-periodic control signal u, where $T > 0$, satisfies $u(t+T) = u(t)$ for all $t \ge 0$. Define $\eta_i = \frac{1}{T}\int_0^T u_i(s)\,\mathrm{d}s \in [0,1]$ for each control input i. Because u is T-periodic, $\frac{1}{T}\int_t^{t+T} u_i(s)\,\mathrm{d}s = \eta_i$ for all $t \ge 0$. The value η_i is called the *utilization* of control input i. The utilization vector $\eta \in [0,1]^m$ of all control inputs is defined by stacking their individual utilizations, i.e., $\eta = [\eta_1, \ldots, \eta_m]^T$.

A sufficient schedulability condition can be stated in the following theorem (for details, cf. our technical report [19]). Here the notation $\mathrm{int}\,(\texttt{Safe})$ denotes the interior of set Safe.

Theorem 1: If there exists $\eta \in [0,1]^m$ such that:

1) $\sum_{i=1}^{m} \eta_i \le k$, and
2) $-CA^{-1}(B_0 + B\eta) \in \mathrm{int}\,(\texttt{Safe})$,

then system (5) is k-schedulable.

A similar result was derived in [20] for scheduling LQR controllers under resource constraints, however its objective is performance bound while we consider safety in this paper.

C. Feasible peak constraint

Given system (5), it is usually of interest to find a feasible peak constraint k because k is not known at the beginning. From Theorem 1, the smallest peak constraint $k_{\min}$ can be computed by minimizing $\sum_{i=1}^{m} \eta_i$ subject to $\eta \in [0,1]^m$ and

$$-CA^{-1}(B_0 + B\eta) \in \mathrm{int}\,(\texttt{Safe}), \qquad (6)$$

and letting $k_{\min} = \lceil \sum_{i=1}^{m} \eta_i \rceil$, where the notation $\lceil c \rceil$ denotes the smallest integer not less than c. Any peak constraint $k \ge k_{\min}$ will be feasible. In practice, Safe is usually a hypercube or a polytope, for which constraint (6) becomes linear and the above optimization can be solved efficiently [21].

IV. Periodic control synthesis

In this section, we present a procedure to design periodic control u for system (5) that both satisfies a given feasible peak constraint k and drives the system's output to Safe.

A. Limit behavior under periodic control

It is shown in [19] that as $t \to \infty$, the output trajectory of (5) under periodic control converges to the limit cycle $\hat{y}(t) = \overline{y}^\star + C\hat{\xi}(t)$. Here, $\overline{y}^\star = -CA^{-1}(B_0 + B\eta)$ and $\hat{\xi}(t)$ is the solution of the ordinary differential equation (ODE)

$$\dot{\hat{\xi}}(t) = A\hat{\xi}(t) + B(u(t) - \eta), \quad \hat{\xi}(0) = P\xi(T) \qquad (7)$$

where $P = \left(I - \mathrm{e}^{AT}\right)^{-1}$ (the matrix inverse exists because A is Hurwitz). Furthermore, $\hat{\xi}(t)$ is T-periodic. Therefore, $\hat{y}(t)$ is also T-periodic and can be computed numerically using any available ODE solver.

B. Synthesize periodic control

In synthesizing periodic control for system (5), it is necessary to ensure that the entire limit cycle $\hat{y}(t)$ is inside `Safe`, so that the system's outputs are driven to and stay inside `Safe`. It is usually desirable to construct a periodic control signal u with the largest period T to minimize the switching frequency. Once a feasible peak constraint $k \geq k_{\min}$ is chosen, this is achieved by solving the optimization:

$$\begin{aligned} \text{maximize}_{\eta,T,u(\cdot)} \quad & T \\ \text{subject to} \quad & \eta \in [0,1]^m, \quad \textstyle\sum_{i=1}^m \eta_i \leq k, \quad T > 0 \\ & u(\cdot) \text{ is } T\text{-periodic with utilization } \eta \\ & \textstyle\sum_{i=1}^m u_i(t) \leq k, \quad \forall 0 \leq t \leq T \\ & \hat{y}(t) \in \texttt{Safe}, \quad \forall 0 \leq t \leq T \end{aligned} \tag{8}$$

However, this optimization is difficult because $u(\cdot)$ is infinite dimensional and the limit cycle $\hat{y}(t)$ (constraint (8)) cannot be solved analytically but only numerically. Therefore, we restrict $u(\cdot)$ to a specific form and use a search algorithm to maximize T subject to constraint (8). Following are the steps to synthesize periodic control with a given peak constraint $k \geq k_{\min}$.

Step 1: Compute utilization

Recall that the limit cycle is $\hat{y}(t) = \overline{y}^\star + C\hat{\xi}(t)$. Intuitively, it is desirable to have $\overline{y}^\star$ not only inside `Safe` but also as far as possible from the boundary of `Safe`. Let y_c be the Chebyshev center of `Safe`. Then η is computed by solving the following optimization:

$$\begin{aligned} \text{minimize}_{\eta} \quad & \|\overline{y}^\star - y_c\|_2 = \left\|-CA^{-1}(B_0 + B\eta) - y_c\right\|_2 \\ \text{subject to} \quad & \eta \in [0,1]^m, \quad \textstyle\sum_{i=1}^m \eta_i \leq k \\ & -CA^{-1}\left(B_0 + B\eta\right) \in \text{int}\left(\texttt{Safe}\right) \end{aligned}$$

where the last constraint becomes linear if `Safe` is a hypercube or a polytope.

Step 2: Construct periodic control

Once η has been computed, distribute m non-overlapping right-open intervals, each of length η_i respectively, into the interval $[0, k]$ on the real line (Fig. 2). Let interval i be $[s_i, s_i + \eta_i) \subseteq [0, k]$. Since $\sum_{i=1}^m \eta_i \leq k$, such a distribution is always possible. Given any period $T > 0$, construct the T-periodic $u_i(\cdot)$ as

$$u_i(t) = \begin{cases} 1 & \text{if } (j + r_i)\,T \leq t < (j + r_i + \eta_i)\,T,\ j \in \mathbb{N} \\ 0 & \text{otherwise} \end{cases}$$

in which $r_i = s_i - \lfloor s_i \rfloor \geq 0$, where the notation $\lfloor c \rfloor$ denotes the largest integer not exceeding c. It can be shown that $\sum_{i=1}^m u_i(t) \leq k$ for all t. Notice that when T varies, u keeps the same pattern and is only scaled by T in time.

Step 3: Compute time period T

In this step, we maximize T subject to constraint (8), in which $\hat{y}(t)$ can only be computed numerically. T can be approximated by using a standard binary search algorithm where in each iteration, the limit cycle $\hat{y}(t)$ is computed for $t \in [0, T]$ and is checked whether it is inside `Safe`.

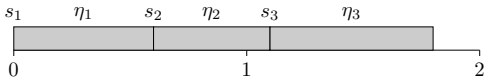


Fig. 2. Distribution of m non-overlapping intervals into $[0, k]$.

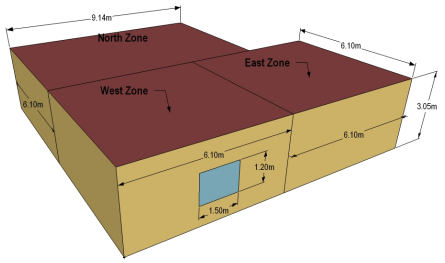


Fig. 3. 3-D Building Model for the small-scale case study.

V. Case Study

In this section we report the results of two case studies in which we applied the proposed green scheduling approach to a multi-zone building with radiant heating system. We also compare the results to uncoordinated On-Off control.

A. Small-scale case study with EnergyPlus

In the first case study, we considered a single floor, L-shaped building divided into 3 interior conditioned zones as shown in Figure 3. There is a single window in the West zone South wall. An electric low temperature radiant system is used for heating the floor of each zone, with power ratings of 12kW, 8kW and 8kW for the North, West and East zones respectively. Temperatures in each zone were desired to be kept between $l = 22\,^\circ\text{C}$ and $h = 24\,^\circ\text{C}$. The ambient air temperature profile was of Chicago, IL, USA. The disturbances due to internal heat gain and solar heat gain were different for every zone and time-varying.

An EnergyPlus model of the building was modified from an example distributed with EnergyPlus 7.0. In this case study, we used the EnergyPlus model as the ground truth for the building, i.e., it was considered as the "real" building. System identification of the building model and implementation of controllers for the building's radiant heating system were carried out in Matlab, while thermal simulation of the building was performed in EnergyPlus.

1) Model identification: Since the internal thermal model of the EnergyPlus model is not accessible from outside EnergyPlus, our first step was to identify a linear model for the building. In particular, we used the state-space model (4) developed in Section II and identified its parameters based on experiment data obtained from simulation of the building in EnergyPlus. Because there are 3 zones in the building, the model has 9 state variables, 3 control inputs, and 3 outputs. The disturbances are the ambient air temperature, the solar radiation, and the internal heat gains for each zone. EnergyPlus were used to run controlled experiments on the building model for 5 days in January and data from EnergyPlus was recorded. The *System Identification Toolbox*

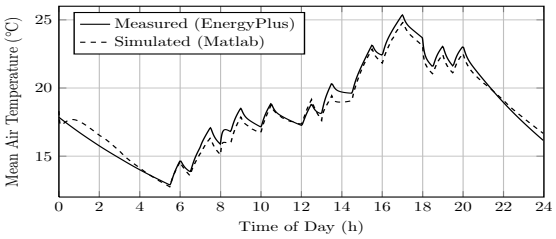


Fig. 4. Validation of the identified model for output 1 (West zone) in the small-scale case study.

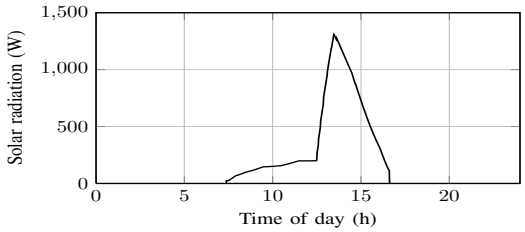


Fig. 5. Predicted solar radiation gain to the West zone in the small-scale case study.

of Matlab was used to estimate the parameters of the model from the experiment data.

Validation of the model was performed on January 14, which is not one of the experiment days. Figure 4 plots the measured (in EnergyPlus) and simulated (in Matlab) mean air temperature of the West zone. The simulation outputs fit the measured outputs 84.24%, 76.89% and 84.26% for the West, East, and North zones respectively.

2) Green scheduling synthesis: We applied the periodic green scheduling approach to the case study on the validation day. The heating schedule of the EnergyPlus model specifies that the heating system is turned off during the night from 6 PM to 6 AM, then is turned on to pre-heat the building from 6 AM to 8 AM, and is in normal operation mode from 8 AM to 6 PM (the working hours of the building). Therefore, we used green scheduling for controlling the radiant heating systems of the building from 8 AM to 6 PM.

Recall that in the system model (5) for green scheduling, we use nominal values for the disturbances. In this case study, disturbance prediction was used to derive these nominal values. According to the weather profile, the ambient air temperature varied around $-6\,^{\circ}\mathrm{C}$ between 8 AM and 6 PM, thus we used $-6\,^{\circ}\mathrm{C}$ as the nominal value for T_a. Based on the occupancy and equipment schedules, the internal heat gain of each zone can be predicted, and we chose its nominal value to be 600 W, 700 W, and 800 W for the West, East, and North zones respectively. For the predicted solar radiation gain to the West zone (the only zone with a window), we noticed a significant increase at around 1 PM due to the window's direction, from under 200 W to over 1000 W (Fig. 5). Therefore, we chose two different nominal solar radiation gains: 100 W before 1 PM and 600 W after 1 PM (both were averaged values for the respective intervals).

On inspecting the predicted disturbances, we decided to synthesize two periodic schedules: one to be used before 1 PM and one after 1 PM. Their parameters are reported in Table II. Notice that the time period T were both 60 minutes, which are reasonably large. Computation time was less than

TABLE II

TWO PERIODIC SCHEDULES FOR THE SMALL-SCALE CASE STUDY

Schedule	k	η	T (minutes)
Before 1 PM	2	$[0.35, 0.42, 0.45]$	60
After 1 PM	1	$[0.05, 0.19, 0.31]$	60

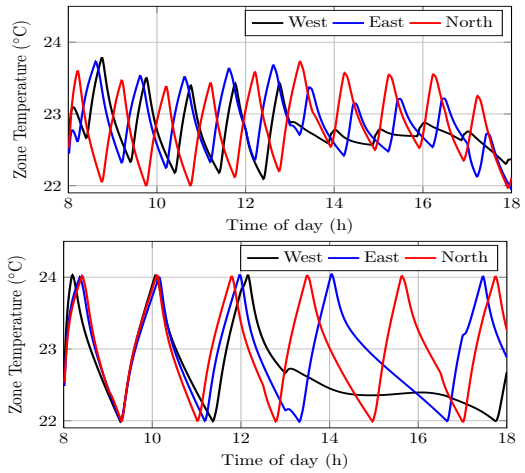


Fig. 6. Zone temperatures for green scheduling (top) and uncoordinated on-off control (bottom) in the small-scale case study.

1 s for each case. Instead of using disturbance prediction, we could monitor the environment (e.g., ambient air temperature, occupancy) and regenerate the schedule on the fly whenever there is a significant change in the disturbances.

3) Simulation results: The periodic schedules were implemented in Matlab and interfaced with the building energy simulation in EnergyPlus. For comparison, we also implemented the uncoordinated on-off control strategy, where the radiant systems were controlled by independent two-position thermostats. Zone temperatures from the simulations are plotted in Fig. 6. In both cases, zone temperatures were kept in the desired range between $22\,^{\circ}\mathrm{C}$ and $24\,^{\circ}\mathrm{C}$. We observed that the electricity demand for the uncoordinated strategy had several high spikes while that of the green scheduling strategy was more flat (Fig. 7). For green scheduling, the effect of switching from the first schedule (peak constraint $k = 2$) to the second schedule (peak constraint $k = 1$) at 1 PM can be seen clearly in Fig. 6 and Fig. 7. In total, green scheduling saved 8% in electricity consumption and reduced peak demand by 42.9% (Table III). This result showed the potential of the proposed approach for reducing peak energy demand. There is a decrease in the total energy consumption since the periodic schedule tends to operate at a lower mean temperature than uncoordinated control (Fig. 6).

B. Large-scale case study

We have seen in the first case study that green scheduling reduced peak demand and flattened the demand curve. The advantage of green scheduling will be shown more clearly

TABLE III

PEAK DEMAND AND CONSUMPTION IN THE SMALL-SCALE CASE STUDY

	Uncoordinated	Green scheduling (% saved)
Consumption (kW h)	93.2	85.7 (8.0%)
Peak demand (kW)	28.0	16.0 (42.9%)

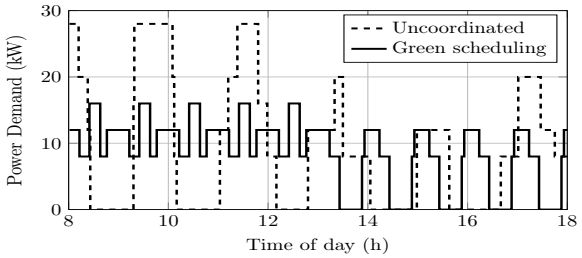


Fig. 7. Electricity demands in the small-scale case study.

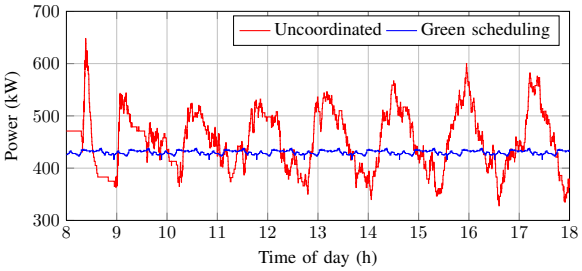


Fig. 8. Electricity demands in the large-scale case study.

when there are a large number of systems to be coordinated. In this case study, we took the identified linear model in the first case study and scaled it to 100 zones. The zones were still coupled, i.e., there were thermal interactions between them. However, unlike the first case study, we simulated the thermal model only in Matlab, not in EnergyPlus because an EnergyPlus model was not available.

Using the same green scheduling synthesis, the peak constraint was computed to be $k = 51$ (among 100) and the time period T was again 60 minutes. The computation in Matlab took only about 3 seconds to complete. We implemented both the green scheduling and the uncoordinated on-off control for comparison. As can be seen on the electricity demand plots in Fig. 8, the demand curve of the green scheduling was almost flat with no sudden spikes, while that of the uncoordinated control had very high peaks repeatedly. The electricity consumption and peak demand of green scheduling were 4303.3 kW h and 438.0 kW, while those of uncoordinated control were 4536.8 kW h and 648.0 kW. Thus green scheduling saved 5.15% in electricity consumption and 32.41% in peak demand, compared to uncoordinated control.

VI. Conclusion

The green scheduling approach for peak power reduction in buildings has been extended to work with electric radiant floor heating systems. The model used in this paper captures the dynamics of actual systems more accurately than in our previous work. We derived sufficient schedulability conditions for general affine dynamical systems and proposed a method for synthesizing periodic schedules for them. Through realistic simulations in EnergyPlus, we showed that our approach is effective for reducing the peak demand of a multi-zone radiant floor heating system. The approach was also shown to be scalable for a large number of zones.

The fast computation time of our method, e.g., about 3 seconds for 100 zones in our case study, allows us to deal with time varying disturbances by recomputing the schedule on the fly when the disturbances change significantly. Since the control signal is on/off, the frequency of switching of the radiant system equipments becomes an important concern. The switching rate depends on how fast the dynamics of the system are and can be controlled. In our case studies, the switching rates were reasonably large (once every hour).

In this work, the thermal inputs to the system were selected from a discrete set, i.e., the control signal (schedule) was only on/off. However, many modern radiant heating systems provide more continuous control options. For future work, we want to look at incorporating continuous control inputs in green scheduling. Hierarchical scheduling algorithms for peak demand reduction in an extremely large-scale system will also be considered.

References

[1] M. H. Albadi and E. F. El-Saadany, "Demand response in electricity markets: An overview," in *Proc. IEEE Power Engineering Society General Meeting*, 2007, pp. 1–5.

[2] TRFund Study, "Understanding PECO's general service tariff," 2007.

[3] B. Olesen, "Radiant floor heating in theory and practice," *ASHRAE Journal*, vol. 44, no. 7, pp. 19–24, 2002.

[4] B. I. Doebber, M. Moore, and M. Deru, "Radiant slab cooling for retail," *ASHRAE Journal*, vol. 52, no. December, pp. 28+, 2010.

[5] Corina and Stetiu, "Energy and peak power savings potential of radiant cooling systems in US commercial buildings," *Energy and Buildings*, vol. 30, no. 2, pp. 127 – 138, 1999.

[6] S. Kiliccote, M. Piette, and D. Hansen, "Advanced controls and communications for demand response and energy efficiency in commercial buildings," in *Second Carnegie Mellon Conf. in Elec. Power Sys.*, 2006.

[7] K. ho Lee and J. E. Braun, "Development of methods for determining demand-limiting setpoint trajectories in buildings using short-term measurements," *Building and Environment*, vol. 43, no. 10, 2008.

[8] Y. Ma, F. Borrelli, B. Hencey, B. Coffey, S. Bengea, and P. Haves, "Model predictive control for the operation of building cooling systems," in *Proc. ACC'10*, 2010, pp. 5106–5111.

[9] F. Oldewurtel, A. Ulbig, A. Parisio, G. Andersson, and M. Morari, "Reducing peak electricity demand in building climate control using real-time pricing and model predictive control," in *Proc. IEEE CDC'10*, 2010, pp. 1927–1932.

[10] F. Tahersima, J. Stoustrup, and H. Rasmussen, "Optimal power consumption in a central heating system with geothermal heat pump," in *Proc. of the 18th IFAC World Congress*. IFAC, 2011.

[11] T.Y. and Chen, "Application of adaptive predictive control to a floor heating system with a large thermal lag," *Energy and Buildings*, vol. 34, no. 1, pp. 45 – 51, 2002.

[12] J.-Y. Lee, M.-S. Yeo, and K.-W. Kim, "Predictive control of the radiant floor heating system in apartment buildings," *Journal of Asian Architecture and Building Eng.*, vol. 1, no. 1, pp. 105–112, 2002.

[13] S.-H. Cho and M. Zaheer-uddin, "An experimental study of multiple parameter switching control for radiant floor heating systems," *Energy*, vol. 24, no. 5, pp. 433 – 444, 1999.

[14] P. Gibbs, "Control of multizone hydronic radiant floor heating system." *ASHRAE Transactions: Part 1*, pp. 1003–1010, 1994.

[15] T. X. Nghiem, M. Behl, R. Mangharam, and G. J. Pappas, "Green scheduling of control systems for peak demand reduction," in *IEEE Conference on Decision and Control (CDC 2011)*, December 2011.

[16] J. Siegenthaler, *Modern Hydronic Heating: For Residential and Light Commercial Buildings*. Cengage Learning, 2011.

[17] J. Seem, *Modeling of heat transfer in buildings*. University of Wisconsin–Madison, 1987.

[18] R. A. Horn and C. R. Johnson, *Matrix analysis*. Cambridge University Press, 1990.

[19] T. X. Nghiem, M. Behl, G. J. Pappas, and R. Mangharam, "Green scheduling for building radiant systems," University of Pennsylvania, Tech. Rep., 2012.

[20] J. Le Ny, E. Feron, and G. J. Pappas, "Resource constrained LQR control under fast sampling," in *Proc. of HSCC '11*. ACM, 2011.

[21] S. Boyd and L. Vandenberghe, *Convex Optimization*, 1st ed. Cambridge University Press, 2006.